Marlou L. Dirks,[1] Benjamin T. Wall,[1] Bas van de Valk,[1] Tanya M. Holloway,[2] Graham P. Holloway,[2] Adrian Chabowski,[3] Gijs H. Goossens,[1] and Luc J.C. van Loon[1]

One Week of Bed Rest Leads to Substantial Muscle Atrophy and Induces Whole-Body Insulin Resistance in the Absence of Skeletal Muscle Lipid Accumulation

Diabetes 2016;65:2862–2875 | DOI: 10.2337/db15-1661

Short (<10 days) periods of muscle disuse, often necessary for recovery from illness or injury, lead to various negative health consequences. The current study investigated mechanisms underlying disuse-induced insulin resistance, taking into account muscle atrophy. Ten healthy, young males (age: 23 ± 1 years; BMI: 23.0 ± 0.9 kg · m^{-2}) were subjected to 1 week of strict bed rest. Prior to and after bed rest, lean body mass (dual-energy X-ray absorptiometry) and quadriceps cross-sectional area (CSA; computed tomography) were assessed, and peak oxygen uptake (VO_2peak) and leg strength were determined. Whole-body insulin sensitivity was measured using a hyperinsulinemic-euglycemic clamp. Additionally, muscle biopsies were collected to assess muscle lipid (fraction) content and various markers of mitochondrial and vascular content. Bed rest resulted in 1.4 ± 0.2 kg lean tissue loss and a 3.2 ± 0.9% decline in quadriceps CSA (both $P < 0.01$). VO_2peak and one-repetition maximum declined by 6.4 ± 2.3 ($P < 0.05$) and 6.9 ± 1.4% ($P < 0.01$), respectively. Bed rest induced a 29 ± 5% decrease in whole-body insulin sensitivity ($P < 0.01$). This was accompanied by a decline in muscle oxidative capacity, without alterations in skeletal muscle lipid content or saturation level, markers of oxidative stress, or capillary density. In conclusion, 1 week of bed rest substantially reduces skeletal muscle mass and lowers whole-body insulin sensitivity, without affecting mechanisms implicated in high-fat diet–induced insulin resistance.

Recovery from injury or illness generally necessitates a period of bed rest, often as a consequence of hospitalization. Prolonged (>10 days) periods of bed rest have been shown to induce substantial changes in body composition and are accompanied by overall metabolic decline (1,2). Though this model of prolonged physical inactivity has taught us much about muscle disuse atrophy, it may be of limited clinical relevance to most patients who are, on average, hospitalized for <7 days (3). Recent data from our laboratory as well as others show that merely a few days of disuse substantially reduces skeletal muscle mass and strength (2,4–6). As a consequence, it has been suggested that the accumulation of such short (<10 days), successive periods of bed rest or immobilization may largely be responsible for the loss of muscle mass and metabolic decline observed throughout the life span (7,8).

Impairments in metabolic health following prolonged disuse have been well described and include a decline in glucose tolerance and insulin sensitivity (1,9), a decrease in resting fat oxidation (10), an increase in mitochondrial reactive oxygen species (ROS) production (11), and a decline in basal metabolic rate (12). As the decline in metabolic health predisposes to greater morbidity and mortality

[1]NUTRIM School of Nutrition and Translational Research in Metabolism, Maastricht University Medical Centre, Maastricht, the Netherlands
[2]Human Health & Nutritional Sciences, University of Guelph, Guelph, Ontario, Canada
[3]Department of Physiology, Medical University of Bialystok, Bialystok, Poland
Corresponding author: Luc J.C. van Loon, l.vanloon@maastrichtuniversity.nl.

Received 15 December 2015 and accepted 23 June 2016.
Clinical trial reg. no. NCT02109380, clinicaltrials.gov.
This article contains Supplementary Data online at http://diabetes.diabetesjournals.org/lookup/suppl/doi:10.2337/db15-1661/-/DC1.
This article is featured in a podcast available at http://www.diabetesjournals.org/content/diabetes-core-update-podcasts.

of patients (13), it is of major clinical relevance to understand the mechanisms responsible for this decline in metabolic health. Prolonged disuse has been associated with substantial loss of muscle mass and/or gain in fat mass (2). Such changes in body composition lower the body's capacity for blood glucose disposal and may contribute to the decline in metabolic health. However, changes in body composition can only partly explain the observed metabolic decline, as reduced insulin sensitivity has been observed during bed rest before measurable changes in body composition became apparent (1,2). We hypothesize that the substantial muscle atrophy caused by short-term bed rest will contribute to, but not fully explain, the vast decline in metabolic health.

One of the key hallmarks of metabolic health is insulin sensitivity. Earlier studies have demonstrated that short periods of bed rest impair glucose tolerance and lower whole-body and/or peripheral insulin sensitivity (14–18). The development of insulin resistance under conditions of lipid oversupply (e.g., type 2 diabetes mellitus and [high-fat] overfeeding) has been associated with lipid deposition in skeletal muscle (19) and, more specifically, with an increase in intramuscular lipid intermediates such as diacylglycerols (DAGs), ceramides, and long-chain fatty acyl-CoA, which impair insulin signaling (as reviewed in Ref. 20). Furthermore, both muscle disuse atrophy (21,22) and the development of insulin resistance (23) have also been attributed to a decline in mitochondrial content and/or impairments in skeletal muscle mitochondrial function. Additionally, impairments in micro- and macrovascular function have been linked to peripheral insulin resistance (24). So far, it is unclear which mechanism(s) contribute to the proposed development of insulin resistance during short-term bed rest.

The objective of the current study was to assess mechanisms that may contribute to the development of insulin resistance during short-term muscle disuse, taking into account the expected muscle atrophy. To achieve this, we subjected healthy, young males to 1 week of strict bed rest and used comprehensive measures of muscle mass and muscle function in combination with detailed metabolic phenotyping (e.g., whole-body insulin sensitivity, substrate metabolism, skeletal muscle lipid content and composition, muscle oxidative capacity, and capillary density) to determine their possible contribution to the development of disuse-induced whole-body insulin resistance. Importantly, this was conducted under energy-balanced conditions to eliminate the contribution of overfeeding to our results. We hypothesized that bed rest–induced insulin resistance is attributed to mechanisms known to induce insulin resistance in chronic metabolic disease (i.e., ectopic lipid deposition, intramuscular accumulation of lipid intermediates, a decline in mitochondrial content and/or impairment in skeletal muscle capillarization). In this study, we demonstrate that short-term bed rest leads to skeletal muscle atrophy, pronounced whole-body insulin resistance, and a decline in skeletal muscle oxidative capacity. Strikingly, these effects do not seem to be mediated via mechanisms involved in obesity-related insulin resistance such as skeletal muscle lipid accumulation, oxidative stress, and micro- and/or macrovascular dysfunction.

RESEARCH DESIGN AND METHODS

Subjects

Ten healthy young men (age 23 ± 1 years) were included in the current study. Subjects' characteristics are presented in Table 1. Prior to inclusion in the study, subjects filled out a general health questionnaire and completed a routine medical screening to ensure their eligibility to take part in the study. Exclusion criteria were a BMI <18.5 or >30 kg · m^{-2}, a (family) history of thrombosis, type 2 diabetes mellitus (determined by HbA_{1c} values >7.0% [53 mmol·mol^{-1}]), and any back, knee, or shoulder complaints. Furthermore, subjects who had been involved in structured and prolonged resistance-type exercise training during the 6 months prior to the study were also excluded. All subjects were informed on the nature and risks of the experiment before written informed consent was obtained. During the screening visit, a fasting blood sample was taken to assess HbA_{1c}, resting energy expenditure was measured with the use of a ventilated hood, and a one-repetition maximum (1RM) estimation test was performed. The current study was approved by the Medical Ethical Committee of Maastricht University Medical Centre (registration number 14-3-013) in accordance with the Declaration of Helsinki.

Experimental Outline

The experimental protocol is depicted in Supplementary Fig. 1. After inclusion into the study, subjects visited the university for a pretesting visit during which the 1RM and peak oxygen uptake (VO_2peak) tests were performed. Following this visit, a 7-day period of standardized nutrition was started. On day 6 of the controlled diet, a mixed-meal tolerance test was performed. The day after, on day 7 of the standardized diet and the day prior to bed rest, test day 1 was scheduled. During this day, a muscle biopsy was taken from the m. vastus lateralis, and a hyperinsulinemic-euglycemic clamp and computed tomography (CT) and dual-energy X-ray absorptiometry (DXA) scans were performed. The next morning, subjects arrived at the laboratory to start the bed rest period. The meal tolerance test was repeated on day 6 of bed rest. After exactly 7 days of bed rest, test day 1 was repeated, and subjects were allowed to

Table 1—Subjects' characteristics

Age (years)	23 ± 1
Body mass (kg)	74.9 ± 2.3
Height (m)	1.81 ± 0.02
BMI (kg · m^{-2})	23.0 ± 0.9
Fasting glucose (mmol · L^{-1})	5.7 ± 0.2
Fasting insulin (mU · L^{-1})	7.2 ± 1.8
HbA_{1c} (% [mmol · mol^{-1}])	5.1 ± 0.1 [32.4 ± 0.9]
RMR (MJ · d^{-1})	7.2 ± 0.2

RMR, resting metabolic rate.

go home. On the next day, subjects returned to the laboratory to repeat the 1RM and VO_2peak tests.

One Week of Bed Rest

To mimic the effects of a standard hospitalization procedure, subjects underwent a 7-day period of strict bed rest. On the morning of day 1, subjects reported to the laboratory in the fasted state at 0800. From that moment on, subjects remained in bed. During the day, subjects were permitted to use a pillow and elevation of the bed-back to perform their daily activities. All hygiene and sanitary activities were performed on the bed. Every morning, subjects were woken at 08 00, and lights were turned off at 2300. Participants were monitored continuously by the research team.

Dietary Intake

During the screening visit, resting energy expenditure was measured by indirect calorimetry using an open-circuit ventilated hood system (Omnical; Maastricht University, Maastricht, the Netherlands) (25). For 7 days prior to bed rest, subjects were given standardized food to prepare and consume at home. During the bed rest period itself, dietary intake was entirely controlled. During the pre–bed rest period, subjects received all food products and prepared the meals at home. In that week, subjects reported to the laboratory once or twice to allow adjustments of the diet in response to body weight changes (when necessary) to keep body weight stable. During bed rest, energy intake was increased when subjects reported being hungry. Energy requirements were estimated based on indirect calorimetry data, multiplied by an activity factor of 1.55 (prior to bed rest) and 1.35 (during bed rest). Macronutrient composition of the diet was identical before and during the bed rest period (Supplementary Table 1).

Body Composition

During test days 1 and 2 (prior to and immediately after bed rest, respectively), anatomical cross-sectional area (CSA) of the quadriceps muscle, hamstrings, and whole thigh were assessed via a single slice CT scan (Philips Brilliance 64; Philips Medical Systems, Best, the Netherlands). While subjects were lying supine, with their legs extended and their feet secured, a 3-mm thick axial image was taken 15 cm proximal to the top of the patella. On test day 1, the precise scanning position was marked with semipermanent ink for replication on test day 2. Next, a single slice CT scan at the level of the upper border of the L3 vertebra was taken to assess total muscle CSA (i.e., all paraspinal and abdominal muscle). For this scan, subjects were lying in a prone position, with their chin resting on both hands. The following scanning characteristics were used: 120 kV, 300 mA, rotation time of 0.75 s, and a field of view of 500 × 500 mm. CT scans were analyzed for the CSA of the whole thigh muscle as well as the quadriceps and hamstring muscles and for total muscle CSA at the level of the L3 vertebra by manual tracing using ImageJ software (version 1.48t; National Institutes of Health, Bethesda, MD) (26). The L3 Skeletal Muscle Index was calculated by dividing the paraspinal muscle area by height squared. Tissue with Hounsfield units between −29 and +150 HU was selected as muscle tissue. The L3 CT scans were also used to determine intramuscular adipose tissue, visceral adipose tissue, and subcutaneous adipose tissue using SliceOmatic software (version 5.0; Tomovision, Montreal, QC, Canada) as described previously (27). Body composition was measured via DXA (Hologic, Discovery A; QDR Series, Bradford, MA). The system's software package Apex version 2.3 was used to determine whole-body and regional lean mass, fat mass, and bone mineral content.

Insulin Sensitivity

On the day prior to bed rest and directly after 1 week of bed rest, a hyperinsulinemic-euglycemic clamp was performed to assess whole-body insulin sensitivity. At the applied level of hyperinsulinemia, hepatic glucose output will be minimal (28,29). Therefore, the presented whole-body insulin sensitivity data presented in this study mainly reflect peripheral insulin sensitivity. Due to the choices for the setup of this experiment, this protocol does not allow assessment of the impact of bed rest on maximal insulin responsiveness. Before the start of the experiment, a Teflon cannula was inserted anterogradely in an antecubital vein of the forearm for the infusion of 20% glucose (Baxter B.V., Utrecht, the Netherlands) and insulin (40 mU $\cdot$ m^{-2} $\cdot$ min^{-1}; Novorapid, Novo Nordisk Farma, Alphen aan den Rijn, the Netherlands). On the contralateral hand, a second cannula was inserted into a superficial dorsal hand vein. From this catheter, arterialized venous blood was obtained by heating the hand in a hot-box (60°C). A small amount of blood was drawn every 5 min throughout the entire 2.5 h clamp to determine glucose concentration (ABL800 Flex; Radiometer Medical, Brønshøj, Denmark). The amount of glucose infused was altered to maintain euglycemia at 5.0 mmol $\cdot$ L^{-1}. The last 30 min of the clamp were used to calculate the mean glucose infusion rate (GIR).

At baseline and during the last 30 min of the clamp, fasting and insulin-stimulated energy expenditure and substrate oxidation were assessed by indirect calorimetry using an open-circuit ventilated hood system (Omnical; Maastricht University, Maastricht, the Netherlands) (25). From these data, total fat and carbohydrate oxidation rates and metabolic flexibility were calculated as described before (30). To test glucose tolerance in a practical manner, a meal tolerance test was performed 2 days prior to bed rest and on day 6 of bed rest at 08:30 as part of the standardized diet. Before and after bed rest, subjects received identical test meals which provided 7.6 ± 0.2 kcal $\cdot$ kg body weight^{-1}, 72 ± 1 g carbohydrate (52 ± 0.4 energy percentage [En%]), 19 ± 0.3 g fat (31 ± 0.4 En%), and 24 ± 0.1 g protein (17 ± 0.2 En%). While subjects were in an overnight fasted state, an antecubital vein was cannulated to allow repeated blood sampling. Prior to breakfast, and at t = 30, 60, 90, and 120 min following meal ingestion, a blood sample was collected in a supine position to assess plasma glucose and insulin concentrations. The disposition index (DI), as a measure of β-cell function, was calculated using the following formula: $DI = (I_{120} - I_0/G_{120} - G_0) \times OGIS$.

Muscle Function Tests

Eight or 9 days before, and on the day after the 7-day bed rest, an incremental cycle ergometer test was performed with 40-W increments every 3 min to determine peak oxygen uptake (VO_2peak). Next, 1RM strength tests on a leg press and leg extension device (Technogym, Rotterdam, the Netherlands) were performed to determine maximal leg strength. The estimations obtained during the screening visit, obtained via the multiple repetitions testing procedure (31), were used to determine 1RM as described previously (32). In short, after warming up, the load was set at 90–95% of the estimated maximum strength and increased after each successful lift until failure. A 2-min resting period was allowed between subsequent attempts. A repetition was deemed valid if the participant was able to complete the entire lift in a controlled manner without assistance. Finally, maximal grip strength was determined using a JAMAR handheld dynamometer (model BK-7498; Fred Sammons, Inc., Burr Ridge, IL). Three consecutive measures were recorded for both hands, and maximal grip strength of both hands was averaged to calculate mean maximal grip strength (33).

Blood and Muscle Sampling

During the meal tolerance tests and on each day of bed rest, blood samples were collected in EDTA-containing tubes and directly centrifuged at 1,000 × *g* for 10 min at 4°C. Aliquots of plasma were snap-frozen in liquid nitrogen and stored at −80°C until further analysis. Additionally, before and after bed rest, a single muscle biopsy was collected from the vastus lateralis muscle. After local anesthesia was induced, a percutaneous needle biopsy was taken ~15 cm above the patella (34). Any visible nonmuscle tissue was directly removed, and part of the biopsy sample was embedded in Tissue-Tek (4583; Sakura Finetek, Zoeterwoude, the Netherlands) before being frozen in liquid nitrogen-cooled isopentane. All remaining muscle tissue was immediately frozen in liquid nitrogen. Muscle samples were subsequently stored at −80°C until further analyses.

Plasma Biochemistry

Plasma glucose and insulin concentrations were analyzed using commercially available kits (GLUC3, reference 05168791 190, Roche; and Immunologic, reference 12017547 122, Roche) (interassay coefficient of variation 4.9% and intra-assay coefficient of variation 1.5%, respectively). Plasma-free fatty acid concentrations were analyzed with an ABX Pentra 400 analyzer (Horiba Diagnostics, Montpellier, France) with test kits purchased from ABX Diagnostics (Montpellier, France).

Skeletal Muscle Analyses

Fiber Typing

Muscle biopsies were stained for muscle fiber typing as described previously (35). The section of the muscle that was mounted and frozen in Tissue-Tek was cut into 5-μm thick cryosections using a cryostat at −20°C. Pre– and post–bed rest samples of each subject were mounted together on uncoated, precleaned glass slides, thereby carefully aligning the samples for cross-sectional fiber analyses. Stainings were performed to analyze muscle fiber-type specific CSA and intramyocellular triglyceride content. To measure fiber type–specific CSA, slides were incubated with primary antibodies directed against myosin heavy chain (MHC)-I (A4.840, dilution 1:25; DSHB) and laminin (polyclonal rabbit antilaminin, L9393, dilution 1:50; Sigma-Aldrich, Zwijndrecht, the Netherlands). After washing, the appropriate secondary antibodies were applied: goat anti-rabbit IgG Alexa Fluor 647 and goat anti-mouse IgM Alexa Fluor 555 (A-21245 and A-21422; dilution 1:400 and 1:500, respectively; Molecular Probes, Invitrogen, Breda, the Netherlands). Myonuclei were stained with DAPI (D1306; 0.238 μmol/L; Molecular Probes). Both primary and secondary antibodies were diluted in 0.1% BSA (A7906; Sigma-Aldrich) in 0.1% Tween 20 (P2287; Sigma-Aldrich) dissolved in PBS. Incubation of antibodies was performed at room temperature. Skeletal muscle tissue was stained as follows. Tissue was fixated in acetone for 5 min, after which the slides were air dried for 15 min and incubated with 3% BSA in 0.1% Tween-PBS for 30 min. Slides were then washed (standard washing protocol: 5 min 0.1% Tween-PBS, 2 × 5 min PBS) and incubated with the first antibodies for 45 min. After washing, slides were incubated with the secondary antibodies, diluted together with DAPI, for 45 min. After a last washing step, cover glasses were mounted by Mowiol (475904-100GM; Calbiochem, Amsterdam, the Netherlands). As a result of the staining procedure, nuclei were stained in blue, MHC-I in red, and laminin in far-red. Images were visualized and automatically captured at ×10 original magnification with a Olympus BX51 fluorescence microscope with customized spinning disk unit (DSU; Olympus, Zoeterwoude, the Netherlands) with a ultra-high sensitivity monochrome electron multiplier CCD camera (1,000 × 1,000 pixels, C9100-02; Hamamatsu Photonics, Hamamatsu City, Japan). Image acquisition was done by Micromanager 1.4 software (36), and images were analyzed with ImageJ (National Institutes of Health). The images were recorded and analyzed by an investigator blinded to subject coding. As a measure of fiber circularity, form factors were calculated by using the following formula: $(4\text{pi} \cdot \text{CSA}) \cdot (\text{perimeter})^{-2}$. On average, 176 ± 31 and 212 ± 60 muscle fibers were analyzed in the pre– and post–bed rest samples, respectively.

Capillary Density

An immunohistochemical staining for skeletal muscle capillarization (Fig. 6*D*) was performed as described previously (37). Slides with muscle cryosections of 5 μm were taken from the −80°C freezer and thawed for 30 min at room temperature. After fixation for 5 min with acetone, samples were air dried again for 15 min. Slides were then incubated for 45 min with CD31 (dilution 1:50; M0823; DakoCytomation, Glostrup, Denmark). Slides were then

washed (standard washing protocol 3 × 5 min PBS). After that, a 45-min incubation step with goat anti-mouse biotin (BA-2000, dilution 1:200; Vector Laboratories, Burlingame, CA) was started, and a standard wash was performed. Next, slides were incubated with Avidin Texas Red (A2006, dilution 1:400; Vector Laboratories) and antibodies against MHC-I (A4.840, dilution 1:25; DSHB) and laminin (polyclonal rabbit antilaminin, dilution 1:50, L9393; Sigma-Aldrich) for 45 min and washed. In the final incubation step, goat anti-mouse IgM Alexa Fluor 488 and goat anti-rabbit IgG Alexa Fluor 350 (A-21042 and A-11046, dilution 1:200 and 1:133, respectively; Molecular Probes) were applied for 30 min. After washing, slides were mounted with Mowiol. The staining procedure resulted in images with laminin in blue, MHC-I in green, and CD31 in red. Images were automatically captured at ×10 original magnification with a Olympus BX51 fluorescence microscope with customized spinning disk unit (DSU; Olympus) with a ultra-high sensitivity monochrome electron multiplier CCD camera (1,000 × 1,000 pixels, C9100-02; Hamamatsu Photonics). Image acquisition was done by Micromanager 1.4 software (36), and images were analyzed with ImageJ (National Institutes of Health). The images were recorded and analyzed by an investigator blinded to subject coding. In all images, a minimum of 30 fibers were counted per fiber type. The number of capillaries was counted and expressed as capillary-to-fiber ratio and capillary-to-fiber perimeter exchange index (CFPE; number of capillaries per 1,000-μm perimeter).

Fiber Type–Specific Lipid Content, Lipid Fractions, and Saturation

An Oil Red O (ORO) staining was performed to analyze muscle fiber type–specific intramyocellular triglyceride content, based on previous work (38). Freshly cut samples were air dried for 30 min and fixated in 3.7% formaldehyde (1040051000; Merck Millipore, Darmstadt, Germany) for 60 min. After rinsing 3 × 30 s with Milli-Q, slides were incubated for 5 min in 0.5% Triton X-100 (108643; Merck Millipore) in PBS. Slides were then washed for 3 × 5 min with PBS and incubated for 45 min with primary antibodies against MHC-I (A4.951, dilution 1:25; DSHB) and laminin (polyclonal rabbit antilaminin, dilution 1:50; L9393; Sigma-Aldrich) in 0.05% Tween-PBS. After washing (1 × 5 min 0.05% Tween-PBS, 2 × 5 min PBS), slides were incubated with the appropriate secondary antibodies: goat anti-mouse IgG1 Alexa Fluor 488 and goat anti-rabbit IgG Alexa Fluor 350 (A-21121 and A-11046; dilution 1:133 and 1:200, respectively; Molecular Probes, Invitrogen). Slides were then washed (1 × 5 min 0.05% Tween-PBS, 2 × 5 min PBS) and rinsed for 30 s with Milli-Q, after which slides were placed in the ORO solution for 30 min. This solution was made by dissolving 250 mg ORO powder (O0625-25G; Sigma-Aldrich) in 50 mL 60% triethylphosphate (538728; Sigma-Aldrich). Of this solution, 48 mL was added to 32 mL of Milli-Q, which was then filtered using a paper-folding filter. After incubation with the ORO solution, slides were rinsed with Milli-Q for 3 × 30 s and placed under slow-running cold tap water before being mounted with cover glasses and Mowiol. The staining procedure resulted in images with laminin in blue, MHC-I in green, and ORO in red. Images were semiautomatically captured at ×40 original magnification with using a Nikon E800 fluorescent microscope coupled with a Nikon DS-Fi1c camera (Nikon Instruments, Amsterdam, the Netherlands) using the NIS-Elements BR software package version 4.20.01. Analysis of the images was done using ImageJ software (National Institutes of Health) by an investigator blinded to subject coding. No differences in fiber circularity were observed between pre– and post–bed rest samples. On average, 34 ± 1 muscle fibers were analyzed in both the pre– and post–bed rest samples. A representative image of the ORO staining is displayed in Fig. 3*A*.

To determine intramuscular lipid content and the degree of saturation, ~50 mg wet muscle was used as described elsewhere (39). Total lipid was extracted using chloroform-methanol (1:1 volume for volume) and internal standards and thereafter evaporated under nitrogen at 37°C. The extracted lipids were separated into triacylglycerol, DAG, free fatty acids (FFA), and phospholipid (PL) by thin-layer chromatography and transferred into separate tubes. After incubation with methanol, pentane was added to the samples, which were then vortexed and centrifuged. The pentane extracts (upper phase) were isolated, and the residues were evaporated under nitrogen at 37°C. Finally, the residues were dissolved in iso-octane, and FA concentrations in the fractions were determined using an analytical gas chromatograph (GC-2010 Plus; Shimadzu, Kyoto, Japan). Muscle ceramide content and ceramide fatty acid species were analyzed as described previously (40).

Enzyme Activities

For mitochondrial enzyme activities, ~10 mg of the muscle was immediately homogenized in 100 volume for weight of a 100 mmol/L potassium phosphate buffer and used for the measurements of maximal β-hydroxyacyl-CoA dehydrogenase (β-HAD) and citrate synthase (CS) activities. Total muscle β-HAD activity was measured in TrisHCl buffer (50 mmol/L TrisHCl, 2 mmol/L EDTA, and 250 μmol/L NADH [pH 7]) and 0.04% Triton-X. The reaction was started by adding 100 μmol/L acetoacetyl-CoA, and absorbance was measured at 340 nm over a 2-min period (37°C) (41). The CS activity was assayed spectrophotometrically at 37°C by measuring the disappearance of NADH at 412 nm (42).

Western Blotting

Muscle was homogenized as previously described (43), 10 μL of protein was loaded, and standard SDS-PAGE procedures were followed. Antibodies included total and phosphorylated Akt (Cell Signaling Technology, Danvers, MA), oxidative phosphorylation (OXPHOS) (MitoSciences, Eugene, OR), vascular endothelial growth factor (VEGF),

hypoxia inducible factor-1α (HIF-1α), endothelial nitric oxide synthase (eNOS), catalase, and superoxide dismutase 2 (SOD2; all Abcam, Cambridge, U.K.), 4-hydroxy-2-nonenal (4-HNE; Alpha Diagnostics, San Antonio, TX), COXIV (Invitrogen), and α-tubulin (Abcam) as a loading control. Protein carbonylation (Oxyblot; Millipore) was determined according to the manufacturer's instructions. Ponceau staining was used to confirm equal loading for antibodies that required the entire membrane (e.g., 4-HNE and protein carbonylation). All samples for a given protein were detected on the same membrane using chemiluminescence and the FluorChem HD imaging system (Alpha Innotech, Santa Clara, CA).

Statistics

All data are expressed as mean ± SEM. Changes over time were analyzed using a paired samples Student *t* test (before vs. after bed rest) or a one-way ANOVA (for daily measurements) using a Bonferroni post hoc test. Muscle characteristics were analyzed using a repeated-measures ANOVA with time (before vs. after bed rest) and fiber type (type I vs. type II) as within-subjects factors. In case of a significant main effect, paired samples *t* tests were performed to assess time effects within fiber types. For the ORO analyses, region (subsarcolemmal vs. intramuscular fat) was added as a within-subjects factor. Statistical significance was set at $P < 0.05$. All data were analyzed using SPSS version 22.0 (SPSS Inc., Chicago, IL).

RESULTS

Body Composition

Figure 1 displays the effect of short-term bed rest on skeletal muscle mass as assessed by DXA (Fig. 1*A*) and CT (Fig. 1*B*). After 1 week of bed rest, participants lost 1.4 ± 0.2 kg (range: 0.6 to 2.8 kg) lean tissue mass (Fig. 1*A*) ($P < 0.01$), representing a 2.5 ± 0.4% loss of lean tissue mass. Lean tissue was mainly lost from the trunk (1.0 ± 0.2 kg) and legs (0.28 ± 0.12 kg) (Table 2). Fat mass did not change during 1 week of bed rest as participants were fed in energy balance (−0.2 ± 0.1 kg; $P > 0.05$). A 3.2 ± 0.9% decline in CSA of m. quadriceps femoris was observed following bed rest (from 7,900 ± 315 to 7,664 ± 354 mm^2; $P < 0.01$) (Fig. 1*B*). CSA of the whole thigh muscle had declined by 2.2 ± 1.0% ($P < 0.05$). CT scans at the level of the L3 vertebra showed a 1.3 ± 0.4% decline in total muscle CSA ($P < 0.01$). As a consequence, the L3 Skeletal Muscle Index had declined from 51.9 ± 2.5 to 51.1 ± 2.4 cm^2 ($P < 0.01$). Analyses performed with SliceOmatic revealed no changes in intermuscular adipose tissue ($P > 0.05$) and visceral adipose tissue ($P > 0.05$). Subcutaneous adipose tissue declined from 93 ± 28 to 89 ± 27 mm^2 ($P < 0.01$). Following bed rest, nonsignificant declines in type I (from 6,650 ± 725 to 6,218 ± 662 μm^2) and type II muscle fiber CSA (from 6,542 ± 746 to 5,982 ± 525 μm^2) were observed ($P > 0.05$) (Supplementary Table 2). No differences in fiber circularity were observed between pre– and post–bed rest samples.

Insulin Sensitivity and Glycemic Control

GIR during the hyperinsulinemic-euglycemic clamp had declined by 29 ± 5% (range 9–53%; $P < 0.01$) following 1 week of bed rest (Fig. 2*A*). Adjustment of GIR for total body weight rather than lean body mass yielded similar results (−29 ± 5%; $P < 0.01$). Postprandial plasma glucose and insulin concentrations observed during the meal tolerance tests are displayed in Fig. 2*C* and *D*. For plasma glucose, the area under the curve (AUC) and incremental area under the curve (iAUC) did not differ between both tests (both $P > 0.05$). In contrast, plasma insulin concentrations showed a significant increase in AUC (from 4,963 ± 779 to 6,944 ± 513 $mU \cdot L^{-1} \cdot min^{-1}$; $P < 0.05$) and iAUC (from 4,213 ± 773 to 5,736 ± 430 $mU \cdot L^{-1} \cdot min^{-1}$; $P < 0.05$) following bed rest. Fasting plasma glucose concentrations (Fig. 2*B*) averaged 5.7 ± 0.2 $mmol \cdot L^{-1}$ prior to bed rest and did not change during the bed rest period ($P > 0.05$). For plasma insulin concentrations (Fig. 2*B*), a significant time effect ($P < 0.001$) was observed such that fasting insulin concentrations had increased from 7.2 ± 1.8 $mU \cdot L^{-1}$ at baseline to 11.8 ± 1.8 $mU \cdot L^{-1}$ after 1 week of bed rest. Consequently, the homeostasis model assessment of insulin resistance (HOMA-IR) index increased from 1.9 ± 0.5 to 3.1 ± 0.5 from day 1 to 8 ($P < 0.01$). The calculated DI was −7,043 ± 11,949 and 16,945 ± 9,972 pre– and post–bed rest, respectively ($P > 0.05$).

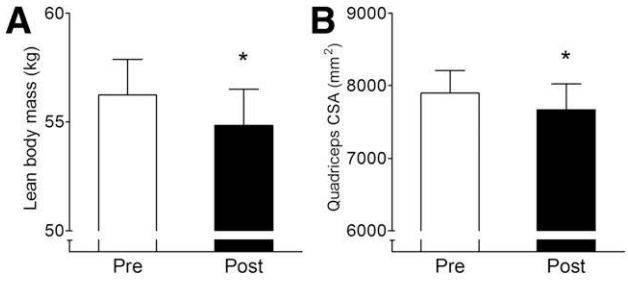

Figure 1—One week of bed rest leads to a substantial decline in muscle mass. *A*: Whole-body lean mass declined by 1.4 ± 0.2 kg following bed rest. *B*: CSA of m. quadriceps femoris declined by 3.2 ± 0.9%. Data represent mean ± SEM. *Significantly different from pre–bed rest value ($P < 0.05$).

Table 2—Body composition

	Pre	Post	*P* value
Total mass (kg)	75.3 ± 2.8	73.7 ± 2.9	<0.001
Total lean mass (kg)	56.2 ± 1.6	54.8 ± 1.7	<0.001
Lean mass trunk (kg)	27.1 ± 0.8	26.1 ± 0.8	0.001
Leg lean mass (kg)	9.6 ± 0.3	9.4 ± 0.3	0.042
Arm lean mass (kg)	3.4 ± 0.2	3.4 ± 0.2	0.183
ALM (kg)	25.9 ± 0.9	25.6 ± 0.9	0.034
SMMI ($kg \cdot m^{-2}$)	7.8 ± 0.2	7.7 ± 0.2	0.026
Total fat mass (kg)	16.3 ± 2.3	16.1 ± 2.3	0.082
Fat percentage (%)	21.2 ± 2.3	21.3 ± 2.3	0.403
BMC (kg)	2.8 ± 0.1	2.7 ± 0.1	0.616

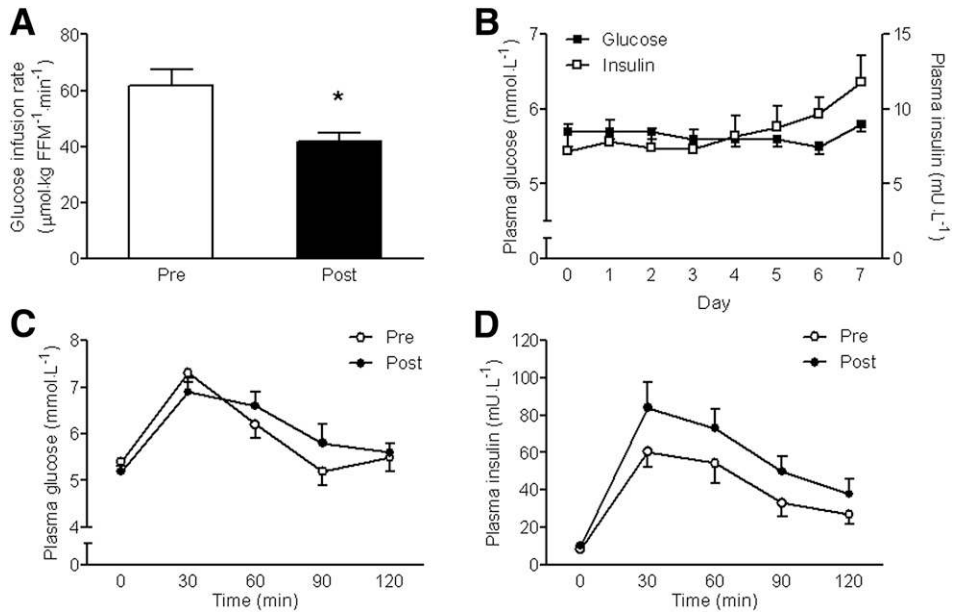

Figure 2— Insulin sensitivity and postprandial glycemic control decline following 1 week of strict bed rest. *A*: Glucose infusion rates declined by 29 ± 5% following bed rest ($P < 0.01$). *B*: Postabsorptive plasma glucose and insulin concentrations on day 1–7 during bed rest. Insulin concentrations increased over time during bed rest ($P < 0.001$). Postprandial plasma glucose and insulin concentrations in the meal tolerance tests pre– and post–bed rest are depicted in *C* and *D*, respectively. For glucose, no changes in iAUC were observed ($P > 0.05$), whereas iAUC for insulin were increased following bed rest ($P < 0.05$). FFM, fat-free mass. Data are shown as mean ± SEM. *Significantly different from pre–bed rest value ($P < 0.05$).

Energy Expenditure and Whole-Body Substrate Oxidation

Resting metabolic rate, as measured by indirect calorimetry, tended to decline from 1,694 ± 47 to 1,624 ± 34 kcal · d^{-1} (−3.8 ± 2.0%; $P = 0.070$) following bed rest. When corrected for the total lean tissue mass, no such trend was observed ($P > 0.05$). During both the pre– and post–bed rest clamps, energy expenditure was increased during insulin infusion (time effect; $P < 0.01$). Stimulation by insulin increased the respiratory quotient from 0.84 ± 0.01 during the baseline period to 0.93 ± 0.01 during exogenous insulin infusion ($P < 0.001$), without differences between pre– and post–bed rest values. Additionally, carbohydrate oxidation rates were increased during the pre– and post–bed rest clamp (baseline: 0.13 ± 0.01, hyperinsulinemia 0.24 ± 0.01 g · min^{-1}; $P < 0.001$). Fat oxidation rates decreased from 0.056 ± 0.007 (baseline) to 0.011 ± 0.005 g · min^{-1} (insulin) during the pre–bed rest clamp and from 0.047 ± 0.004 to 0.014 ± 0.004 g · min^{-1} during the post–bed rest clamp (effect of insulin, $P < 0.001$; trend for *time* × *treatment* effect; $P = 0.065$). Total protein content and phosphorylation status of both Akt (Ser^{473}) and Akt (Thr^{308}), measured in fasted biopsies, were not altered following bed rest ($P > 0.05$).

Functional Outcomes

A significant decline in 1RM leg press strength, from 211 ± 16 to 196 ± 45 kg (−7 ± 1%; $P < 0.01$), was observed following bed rest. Similarly, leg extension strength decreased from 128 ± 7 to 117 ± 7 kg (−8 ± 2%; $P < 0.05$). Following bed rest, no changes in handgrip strength were observed: grip strength averaged 45 ± 2 kg prior to bed rest and 46 ± 2 kg after the 7-day intervention ($P > 0.05$). Results from the cycle ergometer test showed a decline in VO_2peak from 3,332 ± 200 to 3100 ± 162 mL · min^{-1}, representing a 6.4 ± 2.3% loss in VO_2peak following bed rest ($P < 0.05$) at a maximal workload of 260 ± 16 vs 246 ± 15 W, respectively ($P < 0.05$).

Lipid Metabolism

Plasma FFA concentrations (Supplementary Fig. 2) showed a time effect ($P < 0.001$) during bed rest. Post hoc analyses revealed that values on day 7 of bed rest were greater than on days 2 through 5 ($P < 0.05$). At baseline, results from the ORO staining showed a greater lipid area percentage in type I than type II muscle fibers ($P < 0.05$, Fig. 3*B*), with smaller droplets in type I versus type II fibers in the subsarcolemmal region ($P < 0.05$). Following bed rest, no changes in lipid area percentage were observed ($P > 0.05$). Droplet size (Fig. 3*C*) changed, such that a significant *time* × *fiber type* interaction was found ($P < 0.01$). Based on this interaction, we showed greater lipid droplets in type I versus type II fibers following bed rest ($P < 0.01$). Skeletal muscle lipid content of the measured lipid pools did not change with bed rest (all $P > 0.05$, Fig. 4). In the PL pool, the percentage saturation increased ($P < 0.05$) (Supplementary Table 3). For the three other pools, the proportion of polyunsaturated fatty acids increased or tended to increase. Although contents of some specific fatty acid species was altered following bedrest, no changes in total contents of any of the measured lipid pools were observed (Supplementary Table 4).

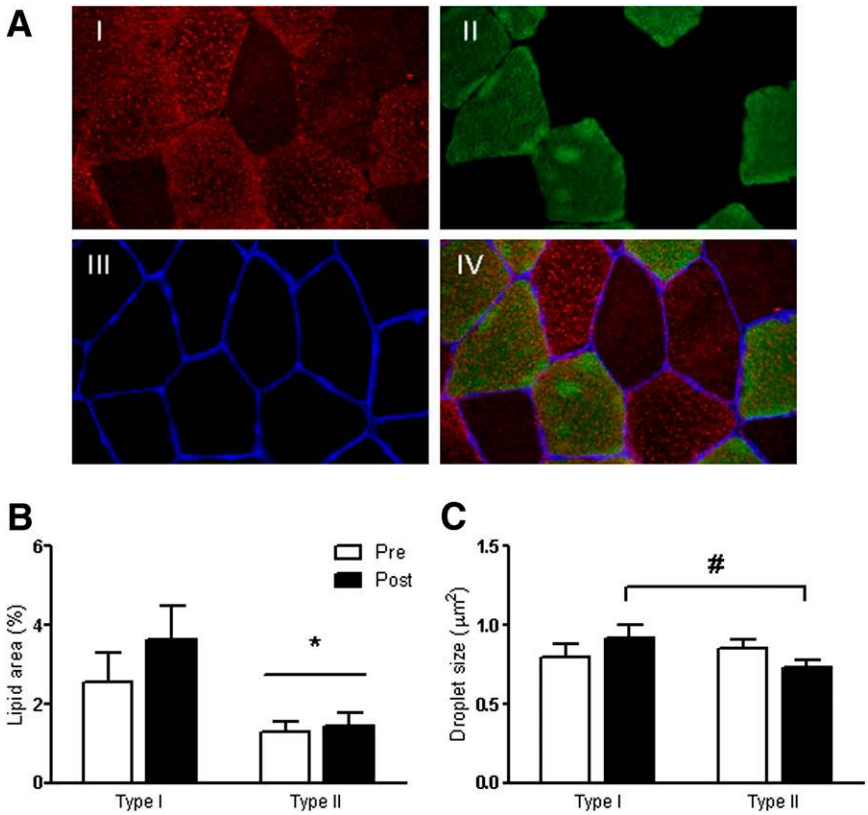

Figure 3—Skeletal muscle lipid contents prior to and following 1 week of bed rest in healthy, young males. Values represent mean ± SEM. *A* represents an image of the ORO staining, made by immunofluorescence microscopy with a magnification of ×40. *I*: ORO. *II*: MHC-I. *III*: Laminin. *IV*: Combined image. The lipid area percentage is depicted in *B* and lipid droplet size in *C*. *Significantly different from type I fibers ($P < 0.05$). #Significant difference between type I and II post–bed rest values ($P < 0.05$).

Oxidative Capacity

Fig. 5 depicts results on various parameters of mitochondrial content. CS activity (Fig. 5*A*) decreased by 8 ± 3% following bed rest ($P < 0.05$). Activity of β-HAD (Fig. 5*B*) tended to decrease by 9 ± 6% ($P = 0.071$). Protein content of the different complexes of the OXPHOS system all decreased or tended to decrease, as depicted in Fig. 5*C*. Lipid peroxidation, determined by 4-HNE content, did not change following bed rest (Fig. 5*D*) ($P > 0.05$). For protein carbonylation (Fig. 5*E*) content, a trend for a decline was observed ($P = 0.075$). Both SOD2 (Fig. 5*F*) and catalase (Fig. 5*G*) protein expression did not change following 1 week of bed rest ($P > 0.05$).

Vascularization

Seven days of bed rest did not lead to significant changes in VEGF (−13 ± 10%; $P > 0.05$) and eNOS (−12 ± 13%; $P = 0.086$) protein expression (Fig. 6*A* and *C*). For HIF-1α protein expression (Fig. 6*B*), a 35 ± 11% increase was observed following bed rest ($P < 0.05$). Bed rest did not lead to changes in capillary density or oxidative exchange across the muscle bed, as shown by the capillary-to-fiber ratio (Fig. 6*E*) and CFPE index (Fig. 6*F*).

DISCUSSION

In the current study, we observed that merely 1 week of bed rest strongly reduced muscle mass, strength, and physical performance. Bed rest resulted in the onset of severe whole-body insulin resistance and a strong decline in skeletal muscle oxidative capacity, both of which occurred in the absence of lipid accumulation or a decline in capillary density in skeletal muscle tissue.

The impact of prolonged bed rest upon skeletal muscle mass and metabolic health has been studied extensively (1,2). Though the model of prolonged disuse is of substantial scientific importance, it may be of more clinical relevance to study short periods of disuse, as patients are typically hospitalized for up to 7 days (3). Recently, we showed that even 5 days of disuse can lead to a ~4% decline in muscle mass and a concomitant ~9% decline in muscle strength (5). In keeping with this, in the current study, we report a 3.2% decline in quadriceps CSA following 1 week of bed rest (Fig. 1*B*) (2). On a whole-body level, this translated to a 1.4 ± 0.2 kg loss of lean tissue (Fig. 1*A*), which is equivalent to ~200 g lean tissue loss per day. In comparison, it took a group of healthy, young males 12 weeks of progressive resistance-type exercise training to gain the equivalent amount of lean tissue (1.7 kg) (44). Thus, we can lose as much muscle in 1 week of bed rest as we can gain by 12 weeks of intense resistance-type exercise training. Furthermore, the loss of muscle was accompanied by a substantial ~8% decline

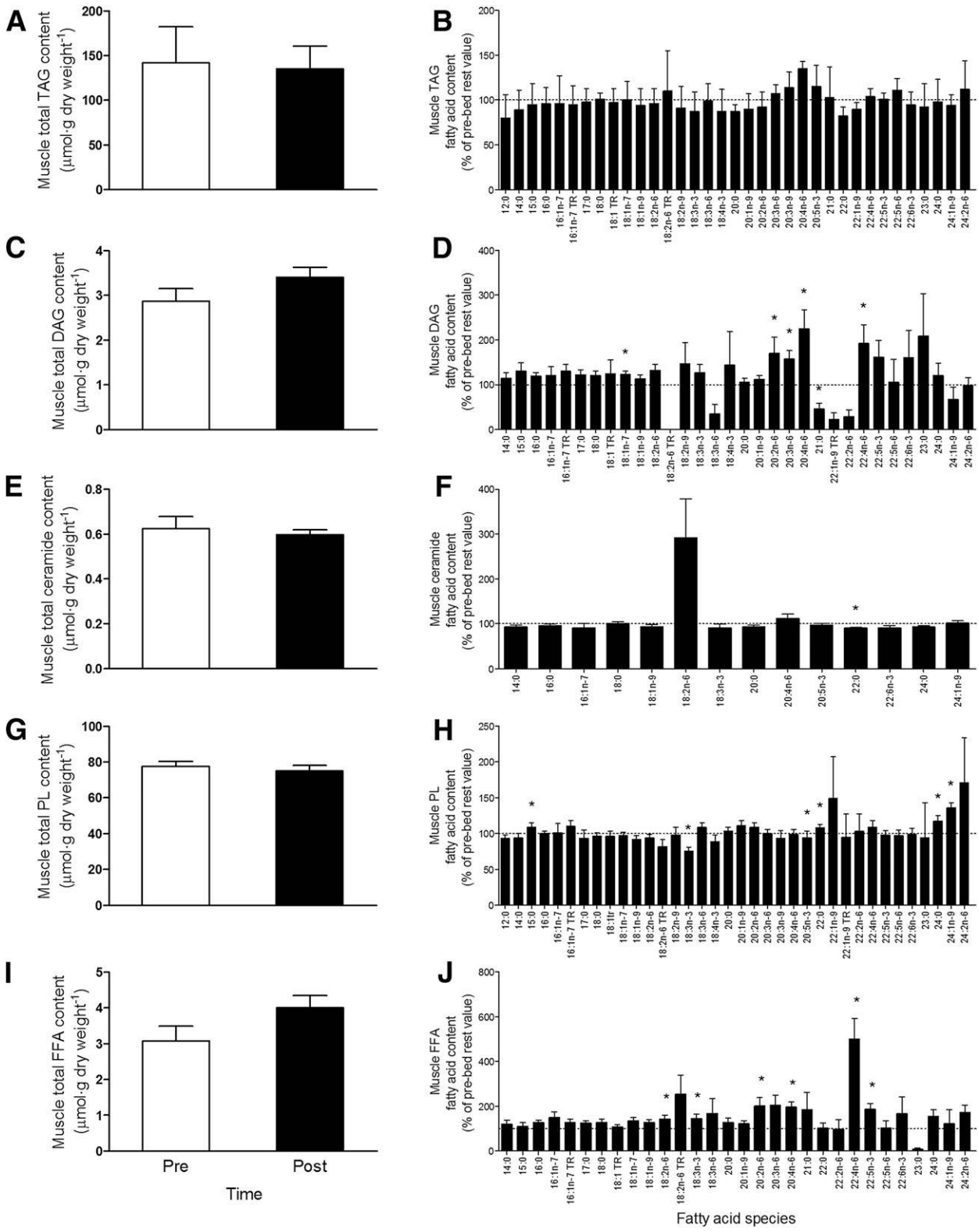

Figure 4—Skeletal muscle total triacylglycerol (TAG) (*A*), DAG (*C*), ceramide (*E*), PL (*G*), and FFA (*I*) content, as well as specific fatty acid species within the different lipid pools. Total content is depicted in the panels on the left, and specific fatty acid species are depicted in panels on the right. Values in *B*, *D*, *F*, *H*, and *J* are expressed as relative change from pre–bed rest values (indicated by the dotted line). *Significantly different from pre–bed rest value ($P < 0.05$).

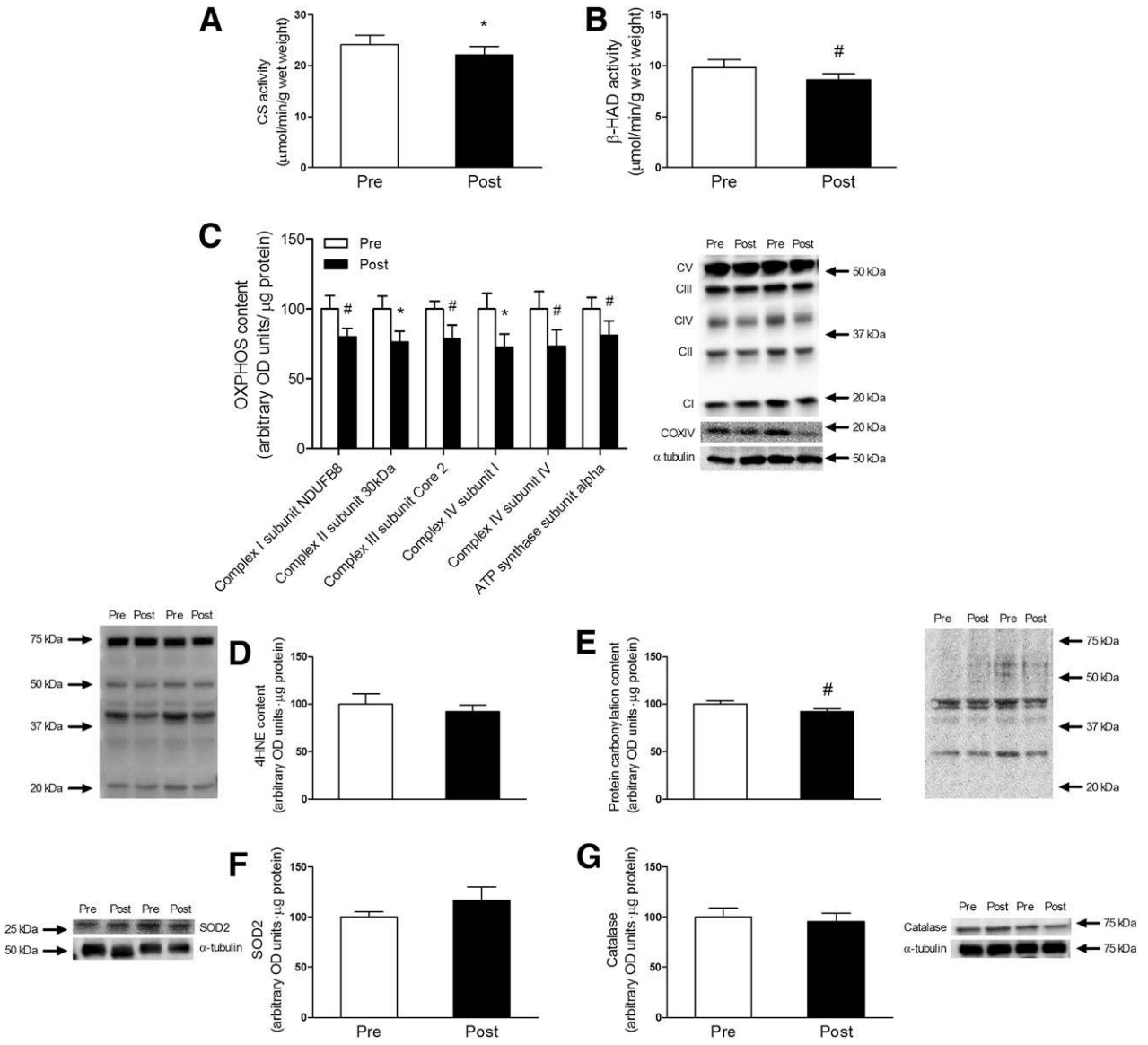

Figure 5—Seven days of strict bed rest leads to a decline in mitochondrial function. CS activity (*A*) decreased ($P < 0.05$), whereas β-HAD activity tended ($P = 0.071$) to decrease (*B*). The protein contents of the different complexes of the oxidative phosphorylation are displayed in *C*. *D*–*G* depict protein expression of 4-HNE, protein carbonylation, SOD2 (predicted molecular weight of 27 kDa), and catalase (60 kDa), respectively. OD, optical density. Data represent mean ± SEM. *Significantly different from pre–bed rest ($P < 0.05$). #Trend for a difference from pre–bed rest value ($P < 0.10$).

in muscle strength and a ~6% reduction in VO_2peak. These findings clearly demonstrate that even a short period of disuse has severe consequences for muscle mass and physical performance, an effect that is unlikely compensated for during rehabilitation. As a consequence, it has been suggested that successive periods of bed rest or immobilization may be responsible for the progressive decline in muscle mass throughout our lifespan (7,8).

The loss of skeletal muscle mass and/or strength during hospitalization has been shown to be predictive of morbidity and mortality (13). This may be more related to the impact of disuse on metabolic health than to the decline in muscle mass per se. Therefore, in the current study, we also aimed to assess the impact of short-term disuse on metabolic health. We performed hyperinsulinemic-euglycemic clamps prior to and after 1 week of bed rest to assess whole-body insulin sensitivity and observed a substantial ~30% decline in glucose disposal (Fig. 2*A*). Under these conditions, hepatic glucose output is strongly diminished, and skeletal muscle is responsible for ~85% of glucose disposal (29). This implies that merely 1 week of bed rest can lower insulin sensitivity by as much as 30%. These findings are in line with previous studies, demonstrating similar declines in whole-body and/or peripheral insulin sensitivity following 7–9 days of bed rest (14–16,18). This decline in whole-body insulin sensitivity manifested in a greater postprandial insulin response required to maintain normoglycemia following bed

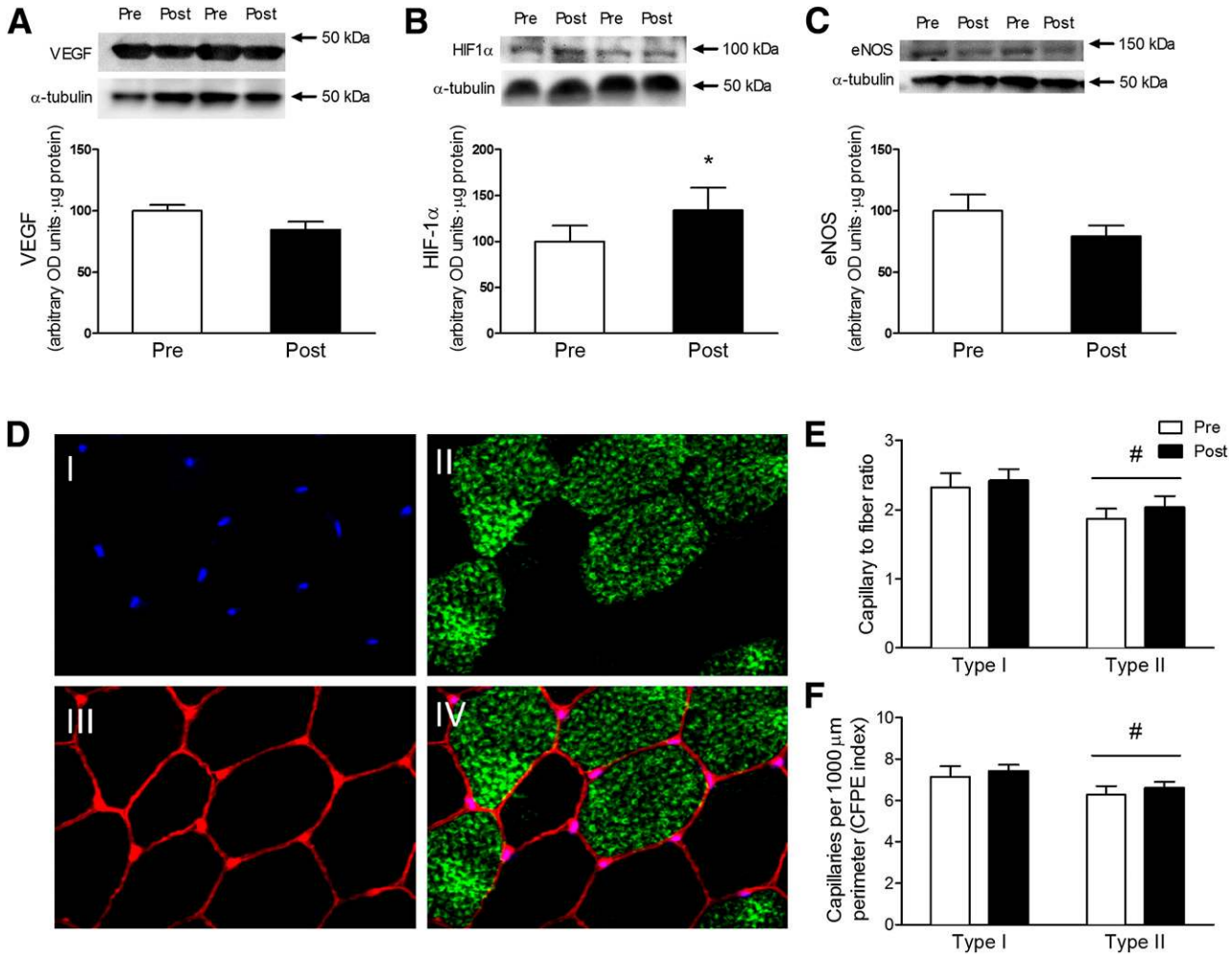

Figure 6—Skeletal muscle capillary content is not altered following short-term bed rest. Values are presented as means ± SEM. No changes in VEGF (*A*, predicted molecular weight 43 kDa) protein expression were observed. A significant increase in HIF-1α (*B*, 97 kDa) protein expression was observed following bed rest. Total eNOS (*C*, 133 kDa) protein expression tended to decline following 1 week of bed rest ($P = 0.086$). *D* represents an immunohistochemical image of the CD31 staining, made by microscopy with a magnification of 20×. *I*: CD31. *II*: MHC-I. *III*: Laminin. *IV*: Combined image. No changes in capillary-to-fiber ratio (*E*) or CFPE index (*F*) were observed. OD, optical density. *Significantly different from values prior to bed rest ($P < 0.05$). #Significantly different from type I fibers ($P < 0.05$).

rest (Fig. 2*C* and *D*), illustrating the impact of physical inactivity on day-to-day metabolic control. Supporting the concept that profound insulin resistance manifested with bed rest, relatively insensitive population markers such as the HOMA-IR index also increased during the intervention. Interestingly, the increase in HOMA-IR over time did not occur until 4 days of bed rest and was entirely attributed to an increase in postabsorptive insulin concentrations (Fig. 2*B*). Thus, it could be suggested that disuse-induced insulin resistance occurs even more rapidly than 1 week (9). Previous work aiming to elucidate the impact of bed rest on insulin signaling has shown that bed rest induced insulin resistance is accompanied by reductions in the contents and/or activity of key proteins regulating glucose uptake and storage in muscle, such as GLUT4, hexokinase 2, and glycogen synthase (18). However, the decline in insulin sensitivity following bed rest could not be explained by impaired insulin and AMPK signaling, as Akt and AS160 signaling seemed to remain intact following short-term bed rest (45). Consequently, other mechanisms are likely to be responsible for the development of insulin resistance following short-term bed rest.

Despite substantial muscle atrophy, a ~3% decline in lean mass likely cannot explain the observed ~30% decline in whole-body insulin sensitivity. As such, during short-term disuse, other mechanisms must contribute to the development of whole-body insulin resistance. Ectopic lipid deposition has often been suggested to lead to the development of insulin resistance in situations of lipid oversupply (19). Although previous studies have reported increases in intramuscular lipid deposition following prolonged bed rest (1), the impact of short-term disuse on skeletal muscle lipid accumulation has been comparatively underinvestigated (46). In line with our previous findings (46), in the current study, we did not detect a measurable

increase in type I or II muscle fiber lipid content (Fig. 3*B*). We extend on these findings by reporting no increase in subsarcolemmal lipid depots, which have been suggested to more specifically contribute to the development of insulin resistance (47). Of course, it could be speculated that an intracellular increase in specific fatty acid intermediates, such as DAGs, fatty acyl-CoA, ceramides, and/or free fatty acids may be responsible for impairments in insulin receptor function and glucose trafficking (20). Therefore, we also measured muscle lipid content of various lipid fractions (Fig. 4). In line with our fiber type–specific data, we did not observe changes in lipid content of the various lipid fractions, including DAGs, following 1 week bed rest. Whereas we did see changes in some specific DAG species (Supplementary Table 4), these were not the 18:2 species that have been specifically linked to insulin resistance (48). Whereas previous work has been inconclusive about the role for ceramides in the development of insulin resistance (49–51), we demonstrate no change in total content and only minor changes in specific fatty acid species within the ceramide pool following bed rest, thereby likely ruling out a mediating role for ceramides in the development of insulin resistance during bed rest. Furthermore, the degree of saturation of specifically the DAG pool has been reported to be increased in insulin-resistant men when compared with control subjects (52). However, we failed to observe any changes in the degree of saturation of the various lipid pools, but actually observed a relative increase in polyunsaturated fatty acids (Supplementary Table 3) in the different lipid pools. This can potentially be explained by a preferential oxidation of saturated fatty acids during disuse, which has been suggested previously (10). Collectively, changes in lipid content and/or lipid composition in skeletal muscle tissue following bed rest are unlikely to explain the observed development of insulin resistance, and therefore other processes must be implicated.

Mitochondrial dysfunction, and specifically the release of mitochondrial ROS, has been postulated as a key factor in the development of muscle disuse atrophy (23) and insulin resistance (53,54). Indeed, previous disuse studies have demonstrated a decrease in mitochondrial protein content and enzyme activities, the onset of mitochondrial respiratory dysfunction, and an increase in ROS emission in situations of muscle atrophy (11,22,55,56). In keeping with this, we show a tendency for a decline in β-HAD (Fig. 4*B*) and a significant 8% decline in citrate synthase activity (Fig. 4*A*), indicative of a decline in mitochondrial content (57). Similarly, protein content of all complexes of OXPHOS (Fig. 4*C*) decreased with bed rest. Given the lack of a fiber-type shift away from oxidative fibers (Supplementary Table 2) that is normally observed following prolonged bed rest, these changes cannot be explained by differences in fiber-type distribution. Additionally, it has been suggested that short-term bed rest could lead to oxidative stress, which in turn triggers the imbalance between muscle protein synthesis and breakdown (58). However, we did not find increases in either 4-HNE or protein carbonylation, suggesting the absence of overt oxidative damage. These findings are in contrast to a previous report analyzing markers of oxidative damage following a longer period of bed rest (59), suggesting that oxidative damage is a consequence of longer periods of bed rest. Given these data, it was not surprising that no changes in the antioxidants superoxide dismutase 2 (SOD2) and catalase (Fig. 4*F* and *G*) were found, as they would usually be increased in the presence of oxidative stress. Previous work by Abadi et al. (22) indicates that muscle oxidative capacity is impaired following short-term disuse. We extend these findings by confirming actual declines in muscle oxidative capacity following bed rest and suggest that, despite not having measured the glutathione/oxidized glutathione ratio to assess short-term redox status, overt oxidative stress does not seem to play a role in the rapid development of insulin resistance during up to 1 week of bed rest. Although time-course studies are clearly warranted to look at instigating factors of muscle atrophy and the rapid development of insulin resistance, our data suggest that impairments in oxidative capacity may (partly) contribute to the observed decline in insulin sensitivity during short-term bed rest.

As in vivo peripheral insulin sensitivity can also be modulated by changes in macro- and microvascular function (60), we also evaluated the effect of bed rest on various angiogenic markers by measuring the expression of VEGF and eNOS, as well as HIF-1α. These data suggest potential early adaptive responses following 1 week of bed rest, as the expression of eNOS tended to decrease, whereas an increase in HIF-1α was seen (Fig. 5). However, this did not result in actual changes in skeletal muscle capillary density as measured by immunohistochemistry. This is in line with previous work showing no changes in capillary density following bed rest (16,55). Consequently, our data do not provide evidence that a decline in capillary networks contributes to the rapid decline in whole-body insulin sensitivity that was observed following 1 week of bed rest.

The magnitude of changes that we observed following merely 1 week of bed rest underlines the impact of short-term muscle disuse, as this study demonstrates that 1 week of bed rest can result in a similar amount of muscle mass and strength loss as can be regained within months of intense rehabilitation (35,44). These changes in lean mass and muscle strength were observed despite our participants being in energy balance, suggesting that the impact of bed rest in undernourished individuals will be even greater. Next to the decline in muscle mass and function, the observed loss in metabolic health during disuse is of paramount importance. By means of comparison, the measured decline in insulin sensitivity (i.e., ~30%) is similar to the difference between a normal glucose-tolerant individual and a patient with type 2 diabetes (52), and is equivalent to a decline that is observed following ~30–40 years of aging (23,61). As the decline in muscle mass, strength, and peripheral insulin sensitivity have been shown

to be good proxy markers for patient outcomes following hospitalization (62), our results emphasize the importance of finding practical and effective interventional strategies that can be applied immediately following the onset of muscle disuse.

We conclude that short-term muscle disuse leads to substantial declines in muscle mass and function and is associated with the development of peripheral insulin resistance and a decrease in skeletal muscle oxidative capacity. Whereas we are still unclear on the molecular mechanisms responsible, our findings clearly indicate that intramuscular lipid accumulation (implicated in high-fat diet–induced insulin resistance), impairments in mitochondrial function and changes in capillary density in skeletal muscle tissue cannot be held responsible for the rapid onset of insulin resistance during a short period of bed rest. Clearly, early interventions are warranted to prevent or attenuate the negative functional and metabolic consequences of short-term bed rest.

Acknowledgments. The authors thank the participants in this study for their enthusiasm and dedication. The authors also thank Wendy Sluijsmans and Hasibe Aydeniz (both part of NUTRIM School of Nutrition and Translational Research in Metabolism) for technical expertise during the muscle analyses and Imre Kouw, Irene Fleur Kramer, Kirsten van der Beek, Jorn Trommelen, Jean Nyakayiru, Philippe Pinckaers, Rinske Franssen, Armand Linkens, Kevin Paulussen, Evelien Backx, and Chantal Strijbos (all part of NUTRIM School of Nutrition and Translational Research in Metabolism) for the practical assistance.

Duality of Interest. No potential conflicts of interest relevant to this article were reported.

Author Contributions. M.L.D. designed the study, organized and performed the experiments, performed the muscle analyses, analyzed the data, interpreted the data, drafted the manuscript, and edited and revised the manuscript. B.T.W. designed the study, organized and performed the experiments, interpreted the data, and edited and revised the manuscript. B.v.d.V. organized and performed the experiments and interpreted the data. T.M.H. and A.C. performed the muscle analyses and interpreted the data. G.P.H. performed the muscle analyses, interpreted the data, and edited and revised the manuscript. G.H.G. designed the study, organized and performed the experiments, interpreted the data, and edited and revised the manuscript. L.J.C.v.L. designed the study, interpreted the data, and edited and revised the manuscript. All authors approved the final version. M.L.D. is the guarantor of this work and, as such, had full access to all the data in the study and takes responsibility for the integrity of the data and the accuracy of the data analysis.

References

1. Bergouignan A, Rudwill F, Simon C, Blanc S. Physical inactivity as the culprit of metabolic inflexibility: evidence from bed-rest studies. J Appl Physiol (1985) 2011;111:1201–1210

2. Wall BT, van Loon LJ. Nutritional strategies to attenuate muscle disuse atrophy. Nutr Rev 2013;71:195–208

3. Statistics Explained. Hospital discharges and length of stay statistics [article online], 2015. Available from http://ec.europa.eu/eurostat/statistics-explained/index.php/Hospital_discharges_and_length_of_stay_statistics. Accessed 17 February 2016

4. Dirks ML, Wall BT, Nilwik R, Weerts DH, Verdijk LB, van Loon LJ. Skeletal muscle disuse atrophy is not attenuated by dietary protein supplementation in healthy older men. J Nutr 2014;144:1196–1203

5. Dirks ML, Wall BT, Snijders T, Ottenbros CL, Verdijk LB, van Loon LJ. Neuromuscular electrical stimulation prevents muscle disuse atrophy during leg immobilization in humans. Acta Physiol (Oxf) 2014;210:628–641

6. Suetta C, Frandsen U, Mackey AL, et al. Ageing is associated with diminished muscle re-growth and myogenic precursor cell expansion early after immobility-induced atrophy in human skeletal muscle. J Physiol 2013;591:3789–3804

7. English KL, Paddon-Jones D. Protecting muscle mass and function in older adults during bed rest. Curr Opin Clin Nutr Metab Care 2010;13:34–39

8. Wall BT, Dirks ML, van Loon LJ. Skeletal muscle atrophy during short-term disuse: implications for age-related sarcopenia. Ageing Res Rev 2013;12:898–906

9. Yanagibori R, Suzuki Y, Kawakubo K, Makita Y, Gunji A. Carbohydrate and lipid metabolism after 20 days of bed rest. Acta Physiol Scand Suppl 1994;616:51–57

10. Bergouignan A, Schoeller DA, Normand S, et al. Effect of physical inactivity on the oxidation of saturated and monounsaturated dietary Fatty acids: results of a randomized trial. PLoS Clin Trials 2006;1:e27

11. Gram M, Vigelsø A, Yokota T, Helge JW, Dela F, Hey-Mogensen M. Skeletal muscle mitochondrial H2 O2 emission increases with immobilization and decreases after aerobic training in young and older men. J Physiol 2015;593:4011–4027

12. Haruna Y, Suzuki Y, Kawakubo K, Yanagibori R, Gunji A. Decremental reset in basal metabolism during 20-days bed rest. Acta Physiol Scand Suppl 1994;616:43–49

13. Weijs PJ, Looijaard WG, Dekker IM, et al. Low skeletal muscle area is a risk factor for mortality in mechanically ventilated critically ill patients. Crit Care 2014;18:R12

14. Alibegovic AC, Højbjerre L, Sonne MP, et al. Impact of 9 days of bed rest on hepatic and peripheral insulin action, insulin secretion, and whole-body lipolysis in healthy young male offspring of patients with type 2 diabetes. Diabetes 2009;58:2749–2756

15. Stuart CA, Shangraw RE, Prince MJ, Peters EJ, Wolfe RR. Bed-rest-induced insulin resistance occurs primarily in muscle. Metabolism 1988;37:802–806

16. Mikines KJ, Richter EA, Dela F, Galbo H. Seven days of bed rest decrease insulin action on glucose uptake in leg and whole body. J Appl Physiol (1985) 1991;70:1245–1254

17. Sonne MP, Alibegovic AC, Højbjerre L, Vaag A, Stallknecht B, Dela F. Effect of 10 days of bedrest on metabolic and vascular insulin action: a study in individuals at risk for type 2 diabetes. J Appl Physiol (1985) 2010;108:830–837

18. Biensø RS, Ringholm S, Kiilerich K, et al. GLUT4 and glycogen synthase are key players in bed rest-induced insulin resistance. Diabetes 2012;61:1090–1099

19. Krssak M, Falk Petersen K, Dresner A, et al. Intramyocellular lipid concentrations are correlated with insulin sensitivity in humans: a ^{1}H NMR spectroscopy study. Diabetologia 1999;42:113–116

20. Bosma M, Kersten S, Hesselink MK, Schrauwen P. Re-evaluating lipotoxic triggers in skeletal muscle: relating intramyocellular lipid metabolism to insulin sensitivity. Prog Lipid Res 2012;51:36–49

21. Max SR. Disuse atrophy of skeletal muscle: loss of functional activity of mitochondria. Biochem Biophys Res Commun 1972;46:1394–1398

22. Abadi A, Glover EI, Isfort RJ, et al. Limb immobilization induces a coordinate down-regulation of mitochondrial and other metabolic pathways in men and women. PLoS One 2009;4:e6518

23. Petersen KF, Befroy D, Dufour S, et al. Mitochondrial dysfunction in the elderly: possible role in insulin resistance. Science 2003;300:1140–1142

24. Muris DM, Houben AJ, Schram MT, Stehouwer CD. Microvascular dysfunction is associated with a higher incidence of type 2 diabetes mellitus: a systematic review and meta-analysis. Arterioscler Thromb Vasc Biol 2012;32:3082–3094

25. Schoffelen PF, Westerterp KR, Saris WH, Ten Hoor F. A dual-respiration chamber system with automated calibration. J Appl Physiol (1985) 1997;83:2064–2072

26. Strandberg S, Wretling ML, Wredmark T, Shalabi A. Reliability of computed tomography measurements in assessment of thigh muscle cross-sectional area and attenuation. BMC Med Imaging 2010;10:18

27. Veasey Rodrigues H, Baracos VE, Wheler JJ, et al. Body composition and survival in the early clinical trials setting. Eur J Cancer 2013;49:3068–3075

28. Conte C, Fabbrini E, Kars M, Mittendorfer B, Patterson BW, Klein S. Multiorgan insulin sensitivity in lean and obese subjects. Diabetes Care 2012;35:1316–1321
29. DeFronzo RA, Jacot E, Jequier E, Maeder E, Wahren J, Felber JP. The effect of insulin on the disposal of intravenous glucose. Results from indirect calorimetry and hepatic and femoral venous catheterization. Diabetes 1981;30:1000–1007
30. Most J, Goossens GH, Jocken JW, Blaak EE. Short-term supplementation with a specific combination of dietary polyphenols increases energy expenditure and alters substrate metabolism in overweight subjects. Int J Obes 2014;38: 698–706
31. Mayhew JL, Prinster JL, Ware JS, Zimmer DL, Arabas JR, Bemben MG. Muscular endurance repetitions to predict bench press strength in men of different training levels. J Sports Med Phys Fitness 1995;35:108–113
32. Verdijk LB, Koopman R, Schaart G, Meijer K, Savelberg HH, van Loon LJ. Satellite cell content is specifically reduced in type II skeletal muscle fibers in the elderly. Am J Physiol Endocrinol Metab 2007;292:E151–E157
33. Guralnik JM, Ferrucci L, Penninx BW, et al. New and worsening conditions and change in physical and cognitive performance during weekly evaluations over 6 months: the Women's Health and Aging Study. J Gerontol A Biol Sci Med Sci 1999;54:M410–M422
34. Bergstrom J. Percutaneous needle biopsy of skeletal muscle in physiological and clinical research. Scand J Clin Lab Invest 1975;35:609–616
35. Leenders M, Verdijk LB, van der Hoeven L, van Kranenburg J, Nilwik R, van Loon LJ. Elderly men and women benefit equally from prolonged resistance-type exercise training. J Gerontol A Biol Sci Med Sci 2013;68:769–779
36. Edelstein A, Amodaj N, Hoover K, Vale R, Stuurman N. Computer control of microscopes using microManager. Curr Protoc Mol Biol 2010;Chapter 14:Unit14.20
37. Groen BB, Hamer HM, Snijders T, et al. Skeletal muscle capillary density and microvascular function are compromised with aging and type 2 diabetes. J Appl Physiol (1985) 2014;116:998–1005
38. Koopman R, Schaart G, Hesselink MK. Optimisation of oil red O staining permits combination with immunofluorescence and automated quantification of lipids. Histochem Cell Biol 2001;116:63–68
39. Moors CC, Blaak EE, van der Zijl NJ, Diamant M, Goossens GH. The effects of long-term valsartan treatment on skeletal muscle fatty acid handling in humans with impaired glucose metabolism. J Clin Endocrinol Metab 2013;98:E891–E896
40. Beaudoin MS, Perry CG, Arkell AM, et al. Impairments in mitochondrial palmitoyl-CoA respiratory kinetics that precede development of diabetic cardiomyopathy are prevented by resveratrol in ZDF rats. J Physiol 2014;592:2519–2533
41. Bergmeyer HU. *Methods of Enzymatic Analysis.* New York, Academic Press, 1974
42. Danson MJ, Hough DW. Citrate synthase from hyperthermophilic Archaea. Methods Enzymol 2001;331:3–12
43. Herbst EA, Paglialunga S, Gerling C, et al. Omega-3 supplementation alters mitochondrial membrane composition and respiration kinetics in human skeletal muscle. J Physiol 2014;592:1341–1352
44. Snijders T, Res PT, Smeets JS, et al. Protein ingestion before sleep increases muscle mass and strength gains during prolonged resistance-type exercise training in healthy young men. J Nutr 2015;145:1178–1184
45. Mortensen B, Friedrichsen M, Andersen NR, et al. Physical inactivity affects skeletal muscle insulin signaling in a birth weight-dependent manner. J Diabetes Complications 2014;28:71–78
46. Wall BT, Dirks ML, Snijders T, et al. Short-term muscle disuse atrophy is not associated with increased intramuscular lipid deposition or a decline in the maximal activity of key mitochondrial enzymes in young and older males. Exp Gerontol 2015;61:76–83
47. Nielsen J, Mogensen M, Vind BF, et al. Increased subsarcolemmal lipids in type 2 diabetes: effect of training on localization of lipids, mitochondria, and glycogen in sedentary human skeletal muscle. Am J Physiol Endocrinol Metab 2010;298:E706–E713
48. Nowotny B, Zahiragic L, Krog D, et al. Mechanisms underlying the onset of oral lipid-induced skeletal muscle insulin resistance in humans. Diabetes 2013; 62:2240–2248
49. Adams JM 2nd, Pratipanawatr T, Berria R, et al. Ceramide content is increased in skeletal muscle from obese insulin-resistant humans. Diabetes 2004; 53:25–31
50. Bonen A, Jain SS, Snook LA, et al. Extremely rapid increase in fatty acid transport and intramyocellular lipid accumulation but markedly delayed insulin resistance after high fat feeding in rats. Diabetologia 2015;58:2381–2391
51. Sitnick MT, Basantani MK, Cai L, et al. Skeletal muscle triacylglycerol hydrolysis does not influence metabolic complications of obesity. Diabetes 2013;62: 3350–3361
52. Jocken JW, Goossens GH, Boon H, et al. Insulin-mediated suppression of lipolysis in adipose tissue and skeletal muscle of obese type 2 diabetic men and men with normal glucose tolerance. Diabetologia 2013;56:2255–2265
53. Anderson EJ, Lustig ME, Boyle KE, et al. Mitochondrial H2O2 emission and cellular redox state link excess fat intake to insulin resistance in both rodents and humans. J Clin Invest 2009;119:573–581
54. Lee HY, Choi CS, Birkenfeld AL, et al. Targeted expression of catalase to mitochondria prevents age-associated reductions in mitochondrial function and insulin resistance. Cell Metab 2010;12:668–674
55. Ringholm S, Biensø RS, Kiilerich K, et al. Bed rest reduces metabolic protein content and abolishes exercise-induced mRNA responses in human skeletal muscle. Am J Physiol Endocrinol Metab 2011;301:E649–E658
56. Levine S, Nguyen T, Taylor N, et al. Rapid disuse atrophy of diaphragm fibers in mechanically ventilated humans. N Engl J Med 2008;358:1327–1335
57. Larsen S, Nielsen J, Hansen CN, et al. Biomarkers of mitochondrial content in skeletal muscle of healthy young human subjects. J Physiol 2012; 590:3349–3360
58. Powers SK, Kavazis AN, DeRuisseau KC. Mechanisms of disuse muscle atrophy: role of oxidative stress. Am J Physiol Regul Integr Comp Physiol 2005; 288:R337–R344
59. Agostini F, Dalla Libera L, Rittweger J, et al. Effects of inactivity on human muscle glutathione synthesis by a double-tracer and single-biopsy approach. J Physiol 2010;588:5089–5104
60. Lillioja S, Young AA, Culter CL, et al. Skeletal muscle capillary density and fiber type are possible determinants of in vivo insulin resistance in man. J Clin Invest 1987;80:415–424
61. Defronzo RA. Glucose intolerance and aging: evidence for tissue insensitivity to insulin. Diabetes 1979;28:1095–1101
62. van den Berghe G, Wouters P, Weekers F, et al. Intensive insulin therapy in critically ill patients. N Engl J Med 2001;345:1359–1367